

## International Journal of Innovative Research in Science, Engineering and Technology

(An ISO 3297: 2007 Certified Organization)

Vol. 4, Issue 8, August 2015

# UV-Vis Absorption and Structural Studies of Eu<sup>3+</sup> Ions Doped Alkali Zinc Bismuth Borate Glasses

Ramesh Boda<sup>1</sup>, G.Srinivas<sup>1</sup>, D.Komaraiah<sup>1</sup>, Md. Shareefuddin<sup>2</sup>, M.N. Chary<sup>2</sup>, R.Sayanna<sup>2</sup>

Research scholar, Department of Physics, Osmania University, Hyderabad, Telangana, India<sup>1</sup>

Professor, Department of Physics, Osmania University, Hyderabad, Telangana, India<sup>2</sup>

**ABSTRACT** : Glasses with the composition  $x\text{Na}_2\text{O}-15\text{ZnO}-20\text{Bi}_2\text{O}_3-(64-x)\text{B}_2\text{O}_3-1\text{EuO}$  [where  $x=0, 5, 10, 15, 20$  mol %] were prepared by the conventional melt quenching technique. X-ray diffraction studies are carried out, effect on glass transition temperature ( $T_g$ ) were carried out using differential scanning calorimetry (DSC) thermograms, and from Archimedes principle, the density of the samples were estimated. Molar volume was calculated from the density data, and the physical properties are calculated using density, refractive index etc. The structural changes in the borate network and bismuth co-ordination with incorporation of alkaline earth oxide variations and rare earth (EuO) doping were investigated by FT-IR spectroscopic techniques. The optical absorption spectra in UV-Vis region (in the wavelength range 200-1000nm) were recorded at room temperature. Cut-off wavelength, direct, indirect band gap, Urbach energy, Molar refraction ( $R_m$ ), Molar electronic polarizability ( $\alpha_m$ ), reflection loss and refractive index values were evaluated from absorbance data.

**KEYWORDS** - Bismuth borate glass, XRD, UV, FTIR, Density, Molar volume, refractive index.

### I. INTRODUCTION

Glasses containing Bismuthate ( $\text{Bi}_2\text{O}_3$ ) have attracted great attention because of their wide applications in the field of glass-ceramics, thermal and mechanical sensors, reflecting windows, radiation shielding. They can be used as layers for optical and opto-electronic devices [1, 2]. Bismuthate glasses containing alkali oxide act as ionic conductors and possess high conductivity compared to other heavy metal oxide glasses. Among different glass matrices, scientific interest on bismuth borate glasses is attributed to their favorable properties such as rigid physical and chemical stability[1], high refractive index, extensive glass formation range, long infrared cutoff and large third order nonlinear optical susceptibility[7-10], low melting temperature[7,8], high density and high infrared transparency. Bismuth borate glasses are also possessing broad range of applications in the fields of optical fiber amplifiers [1-5,8], thermal and mechanical sensors, laser materials[8], electro-optic switches, optoelectronics and magneto optical devices, reflecting windows, photonic switches and layers for optical and electronic devices etc.

In the present system of glasses alkaline earth zinc bismuth borate (ZNB) glasses doped with Europium oxide, the oxides such as  $\text{Bi}_2\text{O}_3$  is added to get good refractive index for using it in enhancement of other optical properties and ZnO could be found as the network modifiers(NWM) and it is a good additive, the oxygen becomes non-bridging when the divalent cat ion like zinc are incorporated in the glass network with relatively large composition range[7,8] and  $\text{B}_2\text{O}_3$  can be used as the network former (NWF) and is contained in most of the prominent commercial glasses.

### I. MATERIALS AND METHODS

Glass preparation:  $\text{H}_3\text{BO}_3$ ,  $\text{Bi}_2\text{O}_3$ , ZnO and  $\text{Na}_2\text{O}$  with  $\text{Eu}_2\text{O}_3$  as doping were used as the raw materials for preparing the glasses, the raw materials in the powder form were mixed using a mortar and pestle. Each mixture was put in muffle furnace melted in a porcelain crucible at  $1000^\circ\text{C}$  for 3–4 hour in air. The glass melts were stirred occasionally to achieve good homogeneity. The highly viscous melt was cast in to a cylindrically shaped mold of stainless steel. The

# International Journal of Innovative Research in Science, Engineering and Technology

(An ISO 3297: 2007 Certified Organization)

Vol. 4, Issue 8, August 2015

glass produced was annealed at 200°C in a second furnace for 2 hr after which the furnace was switched off and the glass was allowed to cool gradually for 2 hrs.

The X-Ray diffractograms were recorded at room temperature with 0.02/sec scanning rate in the range (100-900) using the Philips X-Ray diffractometer with K $\alpha$  tube target and nickel filter operated at 40 kV, 30mA. . All the x-ray diffractograms were recorded at room temperature. The peak free x-ray diffractograms confirmed [fig.1] the amorphous nature of the prepared glass samples.

The infrared transmittance spectra of the glass samples were recorded at room temperature by using Perkin Elmer Frontier FTIR in the mid-IR range (250-4000cm<sup>-1</sup>) KBr pallet technique was used to record the IR spectra the sample was powdered with 0.3g of KBr in the ratio 2:100 and put in to a 13mm dye and passed with a pressure of 7-10 ton using hydraulic press to obtain transparent pallets of approximate 1mm thickness. The spectra of these pallets were then recorded by using universal sample holder with the resolution of 4 cm-1 and 16 scans per sample. The background removal and baseline correction was done with the help of spectrum 10 software.

The densities of these glass samples were determined at room temperature by the Archimedes principle using xylene as an immersion liquid.

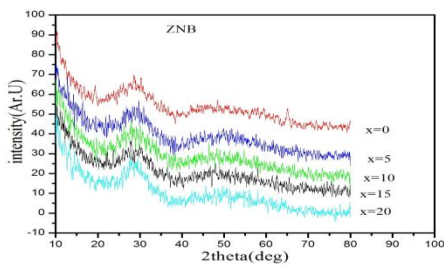


Fig.1.XRD of doped glasses

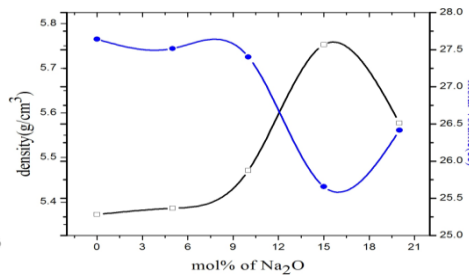


Fig.2.density, molar volume Vs mol % of Na<sub>2</sub>O

The differential scanning calorimetry (DSC) thermograms were recorded using DSC Q20 V24.10 Build 122 Instrument, at the rate of 10.00 °C/min, Equilibrate at 50 °C to 520 °C temperature in Ramp. 3mg of Sample in powder form is taken in to Tzero Aluminium Pan and lid under liquid Nitrogen Gas pressure of 50.0 ml/min.

The optical absorption spectra of the polished samples (optical path length or thickness 2.00mm) were recorded at room temperature using recording spectrophotometer make by Analytical Technologies Limited (Philip halogen, deuterium lamp(200H), model: Spectro UV 2092) in the range 200–1000nm.

## III. RESULTS AND DISCUSSION

### 3.1. Optical absorption

From the Optical absorption spectra we observe eight absorption bands (<sup>5</sup>L<sub>6</sub>, <sup>5</sup>D<sub>3</sub>, <sup>5</sup>D<sub>2</sub>, <sup>5</sup>D<sub>1</sub>, <sup>5</sup>D<sub>0</sub>) and their transitions assigned (fig.3(a)). The cut-off wavelength was evaluated at the absorption edge from (fig.3 (b)). It is clear from the below fig.3 (b). that the absorption edges were not sharp which is an indication of amorphous nature of the glass samples (fig.3).

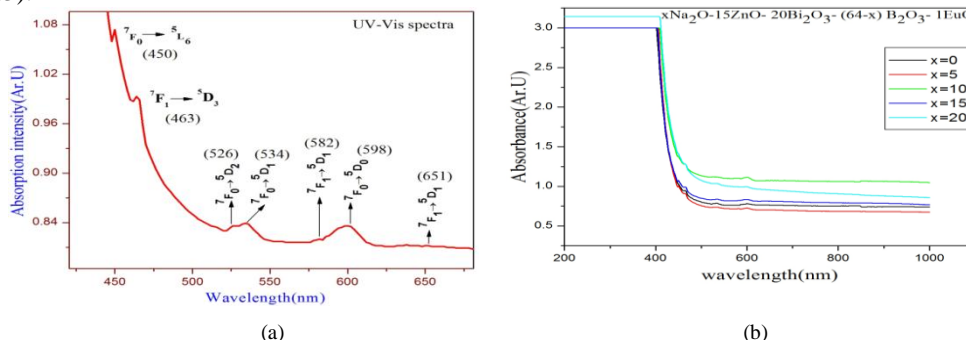


Fig.3.UV-Vis absorption spectra (a) absorption bands and their transitions assigned (<sup>5</sup>L<sub>6</sub>, <sup>5</sup>D<sub>3</sub>, <sup>5</sup>D<sub>2</sub>, <sup>5</sup>D<sub>1</sub>, <sup>5</sup>D<sub>0</sub>) (b) Cut-off wavelengths calculation from absorption edge .

## International Journal of Innovative Research in Science, Engineering and Technology

(An ISO 3297: 2007 Certified Organization)

Vol. 4, Issue 8, August 2015

The absorption coefficient,  $\alpha(\nu)$  is determined near the absorption edge of different photon energies for all glasses and is given by the relation [1, 3];

$$\alpha(\nu) = 2.303 \frac{A}{d}$$

Where 'A' is the absorbance and 'd' is the thickness of the sample and 2.303 is logarithmic conversion factor from log to ln. Davis and Mott proposed the following relation for amorphous materials where the absorption co-efficient  $\alpha(\nu)$  is a function of photon energy ( $h\nu$ ) for direct and indirect transitions [1, 7].

$$(\alpha h\nu) = B^2 (h\nu - E_g)^r$$

Where  $E_g$ , is the optical band gap, and 'r' is the index which has different values (2, 3, 1/2 and 1/3) corresponding to indirect allowed, indirect forbidden, direct allowed and direct forbidden transitions, respectively. B is a constant called the band tailing parameter and  $\nu$  is the energy of incident photons. Here the optical band gap refers to photons assisting the electrons to move from valence band to conduction band. The optical band gap between valence band and conduction band in oxide glasses can be determined from the position of the absorption edge. The absorption edge gives information about the width of the localized states in the band gap which arises due to disorder in the glass matrix. The optical band gap energy also provides information about the nature of chemical bonds and glass structure. The typical  $(\alpha h\nu)^{1/2}$  versus photon energy ( $h\nu$ ) for indirect allowed transitions,  $(\alpha h\nu)^3$  versus ( $h\nu$ ) for direct forbidden,  $(\alpha h\nu)^{1/3}$  versus ( $h\nu$ ) for indirect forbidden and  $(\alpha h\nu)^2$  versus ( $h\nu$ ) direct allowed transitions (called as Tauc's plot) have been plotted to find the values of optical band gap energy,  $E_g$ (fig.4). The values of  $E_g$  are obtained by extrapolating the linear region of the curve to the (x) axis, i.e.  $(\alpha h\nu)^{1/2}=0$  and  $(\alpha h\nu)^2=0$  for indirect and direct transitions and is shown in Figs.4(a),(b). The values of  $E_g$  for absorption edge, indirect allowed transitions and direct allowed transitions are given in Table 1.

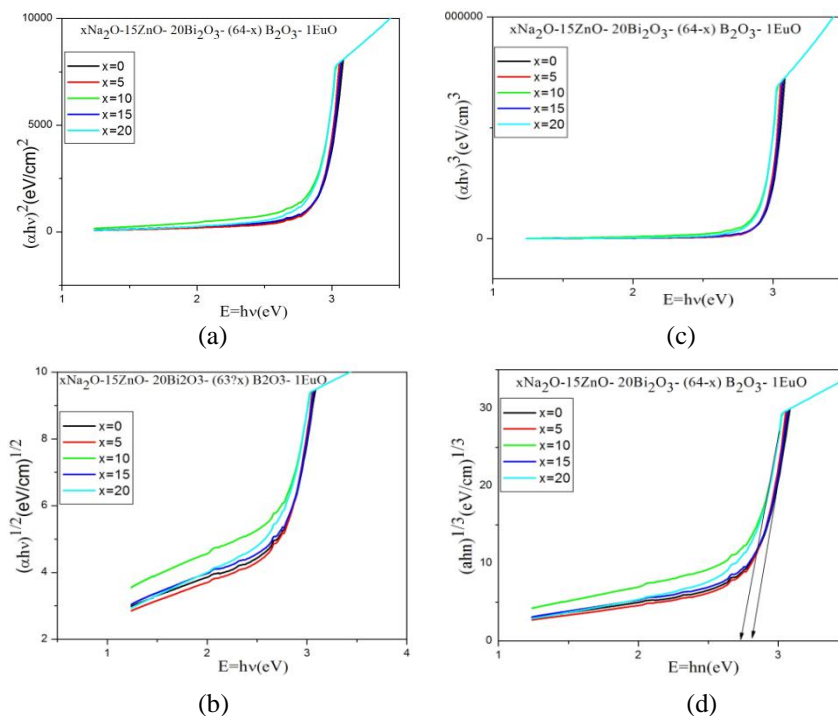


Fig.4: Tauc's plots (a)  $(\alpha h\nu)^2$  versus ( $h\nu$ ) for direct allowed transition (b)  $(\alpha h\nu)^{1/2}$  versus ( $h\nu$ ) for indirect allowed transition (c)  $(\alpha h\nu)^3$  versus ( $h\nu$ ) for direct forbidden transition (d)  $(\alpha h\nu)^{1/3}$  versus ( $h\nu$ ) for indirect forbidden transitions

The value of band gap can be obtained by extrapolating the linear region of  $(a/\lambda)^{1/r}$  versus  $(1/\lambda)$  curve at  $(a/\lambda)^{1/r}=0$ . The x-axis intersect value is multiplied with 1239.83 then it is found that the best fit is observed for  $r=2$ . This value of band gap, designated as  $E_{opt}$  in eV, is calculated from the parameter  $\lambda_g$  using the expression

# International Journal of Innovative Research in Science, Engineering and Technology

(An ISO 3297: 2007 Certified Organization)

Vol. 4, Issue 8, August 2015

$$E_{opt} = \frac{1239.83}{\lambda_g}$$

The variation of  $(\alpha/\lambda)^{1/r}$  verses  $(1/\lambda)$  is used to evaluate the values of optical band gaps  $E_{opt}$  of the present glass samples calculated using ASF method are reported in Table 1. It is observed that the values of optical band gap energy ( $E_g$ ) match the values of optical band gap energies  $E_{opt}$  calculated from ASF method.

### 3.2. Urbach Energy

The Urbach energy,  $\Delta E$  is defined as the energy gap between localized tail states in the forbidden band gap [1]. It provides a measure of disorder in the amorphous and crystalline solids [22]. In amorphous materials, structural disorder dominates and this could be due to the presence of structural defects like dangling bonds or non bridging oxygen atoms [23]. In borate based glass network, the higher the concentration of NBO's, the smaller is the optical band gap energy and the greater are the Urbach energy values [1, 22]. When the energy of the incident photon is less than the band gap, the increase in absorption coefficient is followed with an exponential decay of density of localized states into the gap [23] and the edge is known as the Urbach energy. The lack of crystalline long-range order in amorphous/glassy materials is associated with a tailing of density of states [24]. At lower values of the absorption coefficient ( $\alpha$ ), the extent of the exponential tail of the absorption edge characterized by the Urbach energy is given by [24]

$$\alpha = \alpha_0 \exp\left(-\frac{h\nu - E}{E_u}\right)$$

Where  $E_u$  is Urbach energy, from fig.5 the Urbach energy values are evaluated by taking the reciprocal of the slopes of the linear portion of the curves of  $\ln(\alpha)$  versus  $(h\nu)$  and are listed in Table.1. The variation of Urbach energy ( $\Delta E$ ) with  $\text{Na}_2\text{O}$  concentration is non- linear.

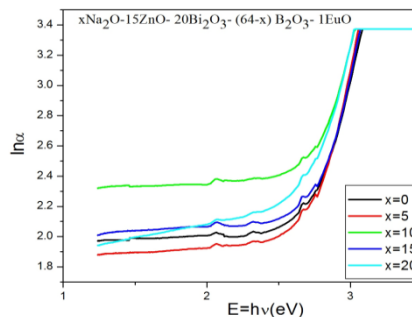


Fig.5: Urbach plots  $\ln\alpha$  verses  $(h\nu)$

Table.1: optical band gap, Cut-off wavelength, Urbach Energy, Reflection loss, Refractive index.

SN	Sample name	Cut-off wavelength	r=1/2	r=1/3	r=2	r=3	Urbach Energy	Ref. loss	Refractive index	$R_m$ ( $\text{cm}^3$ )	$\alpha_m$ ( $10^{24}(\text{\AA}^3)$ )	$T_g$ ( $^{\circ}\text{C}$ )
1	ZNB0	434	2.689	2.772	2.894	2.891	0.223	0.621	2.428	17.693	7.0	462
2	ZNB5	439	2.653	2.74	2.808	2.837	0.236	0.6205	2.432	18.135	7.19	456
3	ZNB10	442	2.627	2.717	2.773	2.797	0.249	0.616	2.411	17.653	6.999	398
4	ZNB15	452	2.569	2.677	2.734	2.734	0.256	0.6212	2.433	18.0	7.137	395
5	ZNB20	459	2.521	2.630	2.709	2.709	0.269	0.6214	2.434	18.0	7.137	363

### 3.3. Refractive Index

Refractive index ( $n$ ) is determined from optical band gap energy ( $E_g$ ) using the formula proposed by Dimitrov and Sakka [38, 39]

# International Journal of Innovative Research in Science, Engineering and Technology

(An ISO 3297: 2007 Certified Organization)

Vol. 4, Issue 8, August 2015

$$\frac{(n^2-1)}{(n^2+2)} = 1 - \sqrt{\frac{E_{opt}}{20}}$$

The refractive index (n) values calculated from above Equation and are given in Table 1. The refractive index values of the present glass samples are in the range 2.411 to 2.434. The refractive index values quoted correspond to the respective values of the present glass samples. However there are chances of creeping small errors in the refractive index "n" values owing to extrapolation ( $a\lambda^{-1}$ )<sup>1/2</sup> verses ( $\lambda^{-1}$ ) plots in estimating  $E_{opt}$ .

### 3.4. Molar refraction ( $R_m$ )

The product of both reflection loss and molar volume is called molar refraction  $R_m$  (cm<sup>3</sup>). This parameter is related to the structure of the glass is given by the Lorentz- Lorentz equation where  $R_m$  is directly proportional to  $V_m$  as follows

$$R_m = \left( \frac{n^2-1}{n^2+2} \right) V_m$$

Where "n" is the refractive index,  $V_m$  is molar volume and the term  $(n^2-1)/(n^2+2)$  represents the reflection loss. The values of molar refraction  $R_m$  are presented in Table.1.

### 3.5. Molar electronic polarizability ( $\alpha_m$ )

According to Clausios-Mosotti, the molar electronic polarizability  $\alpha_m$  is given by the relation

$$\alpha_m = \left( \frac{3}{4\pi Na} \right) R_m$$

where Na is Avogadro's number. The values of molar electronic polarizability  $\alpha_m$  are presented in Table.1.

### 3.6. Infrared spectra

FTIR transmittance spectra [fig.6] showed fine intense absorption bands centred around 1800, 1340, 900, 690, 497 and 280 cm<sup>-1</sup> and small shoulders around 270,300, 352, 1740, 2300, and 3400 cm<sup>-1</sup>. The sharp intense band around 1340 cm<sup>-1</sup> are due to symmetric stretching vibration of B-O bonds in BO<sub>3</sub> units varied from Pyro, Ortho borate groups respectively. A sharp band around 1338, 1344, 1336, 1315, 1313 cm<sup>-1</sup> are due to B-O symmetric stretching vibration in BO<sub>3</sub> units from Pyro and Ortho borate groups, these are highest intensity bands. The sharp band around 690 cm<sup>-1</sup> is due to the bending vibrations of B-O-B units in BO<sub>3</sub> triangles. The broad intense band around 900 cm<sup>-1</sup> is assigned to stretching vibrations of BO<sub>4</sub> units in various structural groups. 2920 cm<sup>-1</sup> and 3020 cm<sup>-1</sup> presence of hydroxyl or water groups present in the glass. The absence of peak at 806 cm<sup>-1</sup> indicates the absence of Boroxol ring in vitreous B<sub>2</sub>O<sub>3</sub> glasses, 883 cm<sup>-1</sup> band is due to Bi-O and /or Bi-O-Bi in [BiO<sub>6</sub>] octahedral. The peak at 704 to 713 cm<sup>-1</sup> is due to B-O-B bending in oxygen bridges between two trigonal boron atoms.

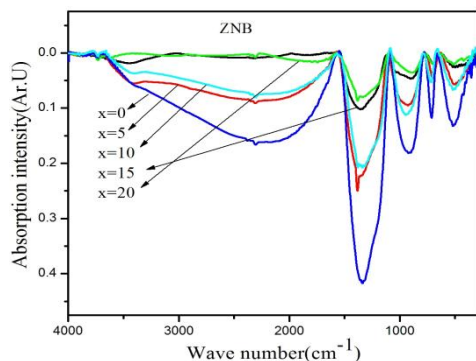


Fig.6. FTIR transmittance spectra

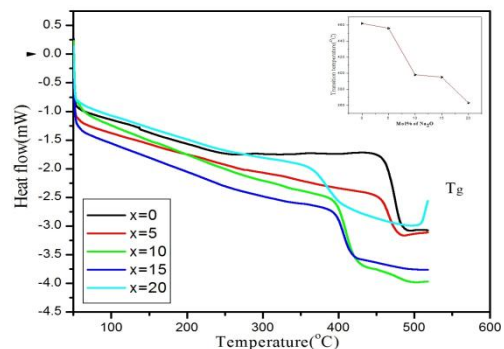


Fig.7.DSC: Temperature Vs heat flow

# International Journal of Innovative Research in Science, Engineering and Technology

(An ISO 3297: 2007 Certified Organization)

Vol. 4, Issue 8, August 2015

Table.2: Observed IR absorption band in  $\text{Eu}^{3+}$  ions doped alkaline earth oxide Zinc bismuth borate glasses.

S No	sample	IR absorption bands							
1	ZNB0	281	497	690	902	1338	1788	2318	3421
2	ZNB5	285	507	698	893	1344	1774	2071	3489
3	ZNB10	270	499	704	902	1336	1840	2312	3408
4	ZNB15	277	543	707	879	1313	1859	2312	3514
5	ZNB20	279	514	709	883	1315	1741	2312	3417

Table.3. Vibration types of different IR wave numbers.

Range of wave numbers ( $\text{cm}^{-1}$ )	Vibration types
270-285	Zn-O vibrations in $\text{ZnO}_4$ units [27, 36]
420-522	Bi-O-Bi stretching vibration of $[\text{BiO}_6]$ octahedral [26, 30]
692-713	Bending vibration of $\text{BO}_4$ units [26, 32, 33]
881-920	Stretching vibration of $[\text{BiO}_3]/[\text{BO}_4]$ units [26, 35, 36]
1317-1363	Stretching vibration of B-O-B in $[\text{BO}_3]$ triangles [26, 30, 33]
1600-1800	Bending modes of OH groups [27, 36]
2304-2380	Anti symmetric stretching of water molecule [28, 37]
2620-2920	Hydrogen bonding [28, 37]
3400-3460	O-H stretching vibration [28, 37]

### 3.7. The DSC

As per the definition of glass the material is said to be glass it should have a transformation temperature called the glass transition temperature in addition to amorphous nature, the values of transition temperatures (table.1) are found to be around 363 to 462 centigrade's from which the glassy nature of samples is confirmed, as the mole percentage of sodium oxide is increasing the transition temperature is decreasing (Fig.7).

### 3.8. Physical properties

The density ( $\rho$ ) values were estimated using the following formula:

$$\rho = \frac{w}{w-w_1} \times \rho_x$$

where  $w$  is the weight of the glass sample in air,  $w_1$  is the weight of the glass sample when immersed in xylene of density ( $\rho_x$ )  $0.865\text{gm/cm}^3$ . The density versus mol% of  $\text{Na}_2\text{O}$  graph gave a non linear relation and the molar volume was calculated from the density data, using the formula

$$V = \frac{M}{\rho}$$

where  $M$  = average molecular weight,  $\rho$ =density.

The molar volume versus mol% of  $\text{Na}_2\text{O}$  graph (fig.2) shows a non linear relation.

The concentration of the rear earth doped ion is calculated using the following formula

$$N_i = \frac{\text{mol \% of dopent} \times \text{Na} \times \text{Density}}{\text{Avg. molecular .wt.}}$$

The polaron radius of the atoms is calculated using the following formula [7-9]

$$R_p = \frac{1}{2} \left( \frac{\pi}{6N_i} \right)^{\frac{1}{3}} A^0$$

Where  $N_i$  is concentration of rear earth ions.

The inter molecular distance is calculated using the following formula [7]

$$R_i = \left( \frac{1}{N_i} \right)^{\frac{1}{3}} A^0$$

Where  $N_i$  is concentration of rear earth ions.

The field strength is calculated from the following formula [7, 8]

$$(f) = \frac{z}{R_p^2} \text{ cm}^{-2}$$

# International Journal of Innovative Research in Science, Engineering and Technology

(An ISO 3297: 2007 Certified Organization)

Vol. 4, Issue 8, August 2015

Where  $R_p$  is polaron radius and  $Z$  is oxidation number.

The dielectric constant is calculated from the refractive index calculated from UV-Vis absorption data and from optical band gap obtained from absorption and is given by [7]

$$\epsilon = n^2$$

Where  $n$  is refractive index.

The Optical dielectric constant is defined as one minus the square of the refractive [7] index i.e.

$$\epsilon_o = n^2 - 1$$

Where  $n$  is refractive index.

The electrical susceptibility ( $\chi$ ) is calculated by formula [7]

$$(n^2 - 1) / 4\pi$$

Table.4: physical properties

S.No	sample	$\rho(\text{g/cm}^3)$	$V_m(\text{cc})$	$\text{Ni}(\times 10^{20})$	$R_p(\text{nm})$	$R_i(\text{nm})$	(f) $(\times 10^{15}\text{cm}^{-2})$	$\epsilon$	$\epsilon_o$	$\chi$
1	ZNB0	5.372	27.641	2.179	0.040	0.153	1.871	5.8854	4.8854	0.3888
2	ZNB5	5.301	28.010	2.150	0.041	0.155	1.822	5.9146	4.9146	0.3912
3	ZNB10	5.379	27.608	2.181	0.040	0.153	1.875	5.8129	4.8129	0.3831
4	ZNB15	5.182	28.657	2.101	0.042	0.159	1.740	5.9195	4.9195	0.3916
5	ZNB20	4.960	29.943	2.011	0.043	0.166	1.594	5.9244	4.9244	0.3919

## IV. CONCLUSIONS

❖ From the XRD studies The glasses of composition  $x\text{Na}_2\text{O}-15\text{ZnO}-20\text{Bi}_2\text{O}_3-(64-x)\text{B}_2\text{O}_3-1\text{EuO}$  shows that the investigated samples are amorphous in nature.

❖ From (DSC) thermograms we confirm that it is glass. From DSC plots, and calculated transition temperature shows that the  $T_g$  is decreasing with increase in the content of  $\text{Na}_2\text{O}$ , and hence decreasing melting temperature.

❖ The FTIR studies revealed that, in the glass matrix, various borate groups are randomly interconnected typical borate groups like ortho borate glasses were observed. From FTIR spectra it is also evident that present glasses consist of pyro, ortho  $\text{BO}_3$  and octahedral  $\text{BiO}_6$  structural units and with increase of  $\text{Na}_2\text{O}$  content the intensity of absorption peaks is decreasing (fig.6) hence we can say that these glasses are more transparent with more content of  $\text{Na}_2\text{O}$ .

❖ From the optical data the evaluated values of optical band gap energy ( $E_g$ ) matches with the values of optical band gap energies  $E_{opt}$  calculated from ASF method. The UV-Vis absorption band is studied and the variation of Urbach energy ( $\Delta E$ ) with  $\text{Na}_2\text{O}$  concentration is varying non-linearly with increase of  $\text{Na}_2\text{O}$  contents.

## V. ACKNOWLEDGEMENTS

One of the authors B.Ramesh is thankful to UGC, New Delhi, for providing financial support, by awarding fellowship under RGNF.

## REFERENCES

- [1] C.R. Kesavulu, K. Kiran Kumar, N. Vijaya, Ki-Soo Lim, C.K. Jayasankar, Materials Chemistry and Physics 141 (2013) 903e911
- [2] D. Ruter, W. Bauhofer, Appl. Phys. Lett. 69 (1996) 892.
- [3] D.A. Turnbull, S.Q. Gu, S.G. Bishop, J. Appl. Phys. 80 (1996) 2436.
- [4] P.E.A. Mobert, E. Heumann, G. Huber, B.H.T. Chai, Appl. Phys. Lett. 73(1998) 139.
- [5] S. Schweizer, L.W. Hobbs, M. Secu, J. Spaeth, A. Edgar, G.V.M. Williams, Appl.Phys. Lett. 83 (2003) 449.
- [6] T. Tsuboi, Eur. Phys. J. Appl. Phys. 26 (2004) 95.
- [7] Xavier Joseph, Rani George, Sunil Thomas, Manju Gopinath, M.S. Sajna, N.V. Unnikrishnan, Optical Materials 37 (2014) 552–560
- [8] X. Feng, S. Tanabe, T. Hanada, J. Am. Ceram. Soc. 84 (2000) 165.
- [9] S.E. Stokowski, M.E. Martin, S.M. Yarema, J. Non-Cryst. Solids 40 (1980) 481.
- [10] C.B. Layne, M.J. Weber, Phys. Rev. B 16 (1977) 3259.
- [11] C.H. Kam, S. Buddhudu, J. Quantitative Spectroscopy & Radiative Transfer 87 (2004) 325–337
- [12] V. Venkatramu, P. Babu, C.K. Jayasankar, Spectrochimica Acta Part A 63 (2006) 276–281

# International Journal of Innovative Research in Science, Engineering and Technology

(An ISO 3297: 2007 Certified Organization)

Vol. 4, Issue 8, August 2015

- [13] K. Swapna, Sk. Mahamuda, A. Srinivasa Rao, T. Sasikala, P. Packiyaraj, L. Rama Moorthy, G. Vijaya Prakash, J. Lumin 156(2014)80–86
- [14] T. Chengaiah, B. C. Jamalaih, L. Rama Moorthy, Spectrochimica Acta Part A: Molecular and Biomolecular Spectroscopy 133 (2014) 495–500
- [15] J. M. Parka, H. J. Kima, Sunghwan Kim, P. Limsuwan, J. Kaewkhao Procedia Engineering 32 (2012) 855 – 861
- [16] S. Surendra Babua, P. Babu, C. K. Jayasankar, W. Sievers, Th. Troster, G. Wortmann, J. Luminescence 126 (2007) 109–120
- [17] K. Upendra Kumar, S. Surendra Babu, Ch. Srinivasa Rao, C. K. Jayasankar, Optics Communications 284 (2011) 2909–2914
- [18] K. Linganna, C. K. Jayasankar, Spectrochimica Acta Part A: Molecular and Biomolecular Spectroscopy 97 (2012) 788–797
- [19] P. Babu, C. K. Jayasankar Physica B. 279 (2000) 262–281
- [20] D. Ramachari, L. Rama Moorthy, C. K. Jayasankar, J. Lumin 143(2013)674–679
- [21] M. Murali Mohan, L. Rama Moorthy, D. Ramachari, C. K. Jayasankar, Spectrochimica Acta Part A: Mol. Bio. Spect. 118 (2014) 966–971
- [22] F. Urbach, Phys. Rev. 92 (1953) 1324.
- [23] B. Abay, H. S. Gudur, Y. K. Yogurtchu, Solid State Commun. 112 (1999) 489.
- [24] M. A. Hassan, C. A. Hogarth, J. Mater. Sci. 23 (1988) 2500.
- [25] M. Mirzayi, M. H. Hekmatshoar, Ionics 15 (2009) 121.
- [26] I. Pal, A. Agarwal, S. Sanghi, M. P. Aggarwal, Optical Materials 34 (2012) 1171–1180
- [27] Joao Coelho, Cristina Freire, N. Sooraj Hussain, Spectrochimica Acta Part A 86 (2012) 392–398
- [28] D. Rajesh, Y. C. Ratnakaram, M. Seshadri, A. Balakrishna, T. Satya Krishna, J. Lumin 132 (2012) 841–849
- [29] I. Arul Rayappan, K. Selvaraju, K. Marimuthu Physica B 406 (2011) 548–555
- [30] S. G. Motka, S. P. Yawale, S. S. Yawale, Bull. Mater. Sci. 25 (2002) 75.
- [31] M. E. Lines, A. E. Miller, K. Nassau, K. B. Lyons, J. Non-Cryst. Solids 89 (1987) 163.
- [32] R. Iordanova, V. Dimitrov, Y. Dimitriev, D. Klissurski, J. Non-Cryst. Solids 180(1994) 58.
- [33] E. I. Kamitsos, A. P. Patsis, M. A. Karakassides, G. D. Chryssikos, J. Non-Cryst. Solids 126 (1990) 52.
- [34] A. K. Hassan, L. Borjesson, L. M. Torell, J. Non-Cryst. Solids 172–174 (1994) 154.
- [35] G. El-Damrawi, K. El-Egili, Physica B 299 (2001) 180.
- [36] S. S. Das, B. P. Baranwal, P. Singh, V. Srivastava, Prog. Cryst. Growth Charact. Mater. 45 (2002) 89–96.
- [37] Cristiane N. Santos, Domingos De Sousa Meneses, Partick Echegut, Daniel R. Neuville, Antonio C. Hernandez, Alain Ibanez, Appl. Phys. Lett. 94 (2009) 151901.
- [38] V. Dimitrov and S. Sakka, I, Journal of Applied Physics, vol. 79, no. 3, pp. 1736–1740, 1996.
- [39] Rajesh Parmar, R. S. Kundu, R. Punia, N. Kishore, and P. Aghamkar, Journal of Materials Volume 2013 (2013), Article ID 650207, 5.